BASIC SCIENCE

Nanomedicine: Nanotechnology, Biology, and Medicine
47 (2023) 102626

Original Article

nanomedjournal.com

Direct quantification of cytosolic delivery of drug nanocarriers using FlAsH-EDT2

R. Rotem, PhD[a,1], J.A. Bertolini, PhD[a,1], L. Salvioni, PhD[a], L. Barbieri, MSc[a], M.A. Rizzuto, PhD[a], V. Tinelli, MSc[a], A. Gori, PhD[b], S. Adams, PhD[c], M. Colombo, PhD[a], D. Prosperi, PhD[a,*]

[a]*University of Milano Bicocca, Milano, Italy*
[b]*Istituto di scienze e tecnologie chimiche, Milano, Italy*
[c]*University of California San Diego, United States of America*

Revised 1 October 2022

Abstract

The delivery of therapeutics across the cell membrane and into the cytoplasm is a major challenge that limits the development of new therapies. This challenge is compounded by the lack of a general assay for cytosolic delivery. Here we develop this assay based on the pro-fluorophore CrAsH-EDT2, and provide cytosolic penetration results for a variety of drug delivery agents (polyethyleneimine, poly-arginine, Ferritin, poly [maleic anhydride-*alt*-isobutene] grafted with dodecylamine, and cationic liposomes) into HeLa and T98G cells. Our results show that this method can be widely applicable to different cells and drug delivery agents, and yield statistically robust results. We later use this method to optimize and improve a model drug delivery agent's (Ferritin) cytosolic penetration.
© 2022 Elsevier Inc. All rights reserved.

Keywords: Quantification method; Cell penetration; Drug delivery; FlAsH-EDT2; Flow cytometry

Introduction

Cytosolic delivery and endosomal escape are critical steps in the delivery of pharmaceuticals to specific intracellular compartments. This is exemplified by the now emerging mRNA vaccines [1,2], anti-inflammatory drugs [3], and cancer therapies [4], to name a few. These steps are limited by drugs and drug delivery agents' ability to cross the cell membrane. The crossing can be achieved through the plasma membrane, or through the membrane of subcellular vesicles, such as endosomes [5–11].

The development of better drug carriers for intracellular targeting is limited by the available methods to measure and quantify this delivery, e.g., discriminating the amount of drug accumulated in the cytoplasm, as opposed to the amount remaining inside the lysosome. Previously published methods included confocal observation of subcellular structures (limited by low throughput and poor statistical significance) [12–15], detection of a biological response to the delivered biological material - e.g., production of GFP following delivery of mRNA (an indirect quantification relying on downstream effects) [12], and detection of specific interactions within specific cellular compartments between endogenic factors and exogenic cargo [16–18]. The ideal method should be specific, fast, and possess high statistical significance, as well as broadly apply to different drug carriers, subcellular compartments, and cells.

Different nanocarriers can be classified according to their mechanism of cell penetration [5,8]. A few investigated mechanisms include the "proton sponge effect", triggered by endosomal acidification of basic, cationic polymers e.g., polyethyleneimine [19] (PEI); the "polymer induced membrane destabilization", triggered by amphiphilic acidic polymers e.g., poly [maleic anhydride-*alt*-isobutene] grafted with dodecylamine (PMDA) [20]; "direct penetration" through the plasma membrane, utilized by short arginine-rich peptides [14] e.g., Arg_{12} (R12), as well as those for which the mechanism is not yet clear, such as H-Ferritin [21] (HFn), among others.

* Corresponding author.
E-mail addresses: Rany.rotem@unimib.it (R. Rotem), davide.prosperi@unimib.it (D. Prosperi).
[1] These authors contributed equally.

https://doi.org/10.1016/j.nano.2022.102626
1549-9634/© 2022 Elsevier Inc. All rights reserved.

Please cite this article as: Rotem R, et al, Direct quantification of cytosolic delivery of drug nanocarriers using FlAsH-EDT2. *Nanomedicine: NBM* 2023;47:102626, https://doi.org/10.1016/j.nano.2022.102626

Here we describe a new method for the quantification of drug nanocarriers' penetration into cells based on the biarsenical profluorophore CrAsH-EDT_2 (carboxy-FlAsH-EDT2) [22–24], that increases its fluorescence when bound to CYS_4, a peptide encoded by a plasmid transiently expressed inside the cell. CrAsH can be covalently conjugated through a free carboxyl group (e.g. to form an amide bond) and the fluorescence resulting from this interaction is then quantified using flow cytometry. We apply this method to different drug carriers and different cells, with high statistical significance.

Results

This work aimed to generate a signal proportional to the degree of cytosolic penetration, based on the interaction of two components: a CrAsH labeled drug carrier, and an endogenic CYS4 peptide inside transfected cells, yielding fluorescent emission in the green region of the spectrum. To help validate and quantify the expression of the CYS4 peptide, it was expressed as a fusion to a blue fluorescent protein, BFP-CYS4. We start by testing each component separately to validate the method.

Proof of concept: cell labeling with a cell-permeable CrAsH analogue, FlAsH-EDT2

HeLa cells were transiently transfected with a plasmids for the expression of either BFP only (predominantly expressed in the cytoplasm and nucleous [25–27]), or a BFP-CYS4 fusion protein, and analyzed using flow cytometry. Fig. 1A and B show the dot plots of the two cellular populations (the position of each dot represents the blue and green emission of a single cell). Fig. 1C shows an average green value for each region of blue intensity (arbitrarily defined as all cells with blue value <600, for the first region, and $600*2^n$ for the limit of the next regions, i.e., 1200 for the 2nd, and 2400 for the 3rd region limit) for both cellular populations. To get a qualitative appreciation of the signal generated from CrAsH-CYS4 binding, the difference (delta) between these lines was plotted, emphasising the emission generated as cell's CYS4 concentration increase and cytosolic CrAsH is activated. In the absence of CrAsH, the difference was negligible. Fig. 1D shows a histogram of the number of cells for each blue region, which is a way to estimate the statistical significance of the data.

After treatment with FlAsH, a cell permeable analogue of CrAsH (Fig. 1E–H), BFP-CYS4 cells show a green-blue dependence, i.e., increased green emission with increased BFP-CYS4 expression indicative of FlAsH activation, contrary to BFP-only cells which show no green-blue dependence. This is qualitatively expressed in the delta line as well. In the case of a NP-CrAsH conjugate taken up by the cell, this delta should follow Eqs. (1)–(6), where I is the measured emission of the cells, I_0 is the exciting light intensity, ε is the extinction coefficient, l is the optical length, QY is the fluorescence quantum yield of CrAsH in the on or off states, and C is the CrAsH concentration in the cytoplasm, everywhere except the cytoplasm (rest), and the total. Accordingly, the delta should be proportional to the nanocarrier concentration in the cytosol, the degree of labelling, and the On/Off emission ratio of CrAsH. The green emission values at the maximal blue (and CYS4) region, from the blue value 614,400 to the saturation value 1,048,580, will later be used as indicators of total cytosolic delivery and delivery ratio (total delivery divided by total association).

$$I_{BFP-only} = 2.303 * I_0 * * l * C^T * QY^{off} + autofluorescence \tag{1}$$

$$I_{BFP-CYS4} = 2.303 * I_0 * \varepsilon * l * \left(C^{cytoplasm} * QY^{on} + C^{rest} * QY^{off}\right) + autofluorescence \tag{2}$$

$$Delta = 2.303 * I_0 * \varepsilon * l * \left(C^{cytoplasm} * QY^{on} + C^{rest} * QY^{off} - C^T * QY^{off}\right) \tag{3}$$

$$C^{rest} = C^T - C^{cytoplasm} \tag{4}$$

$$Delta = 2.303 * I_0 * \varepsilon * l * C^{cytoplasm} * \left(QY^{on} - QY^{off}\right) \tag{5}$$

$$Delta \propto C^{cytoplasm} * \left(\frac{QY^{on}}{QY^{off}} - 1\right) \tag{6}$$

Ex-cellulo activation of nanoparticle-CrAsH

Based on previous reports, we first tested a poly-arginine peptide, termed R12, and its penetration into HeLa cells to improve the chance of measuring a cytosolic signal [14,15].

The R12-CrAsH conjugate was first tested with free CYS4 to validate the emission increase in response to CYS4 binding. The conjugate was incubated in a multi well plate for 1 h at 37 °C in cell medium with 10 μM CYS4 and 8 mM glutathione to resemble the cytoplasm (this was found to have an impact on the On/Off emission ratio of CrAsH through partial non-specific activation of CrAsH). Under these conditions, the On/Off emission ratio was 53 ± 4, with a CrAsH/R12 conjugation ratio of 0.17. Cetuximab-CrAsH (CTX-CrAsH) nanoconjugate, meant to be used as a negative control (i.e., to enable CrAsH labelling of the cell, with negligible endosomal escape), was found to have an On/Off ratio of 6.2 ± 0.7 with a CrAsH/CTX conjugation ratio of 7. The On/Off ratio was probably limited by lower accessibility of CYS4 to CrAsH on-top of the bulkier CTX, as will be evident later for other nanoconjugates as well.

Selection of cell treatment protocol

Using a carboxyfluorescein-conjugated R12 (R12-CF) and CTX (CTX-CF), the time and dosage of each nanoconjugate was selected to maximize each nanocarrier's uptake (Fig. 2A and B), limit the toxicity to the cells as determined by either MTS assay or changes in cells morphology/adhesion, and allow enough time for CrAsH + CYS4 binding inside the cytoplasm [22] (referring to the 1 h incubation in DMEM between R12 treatment and harvesting, see treatment protocol in Table 1).

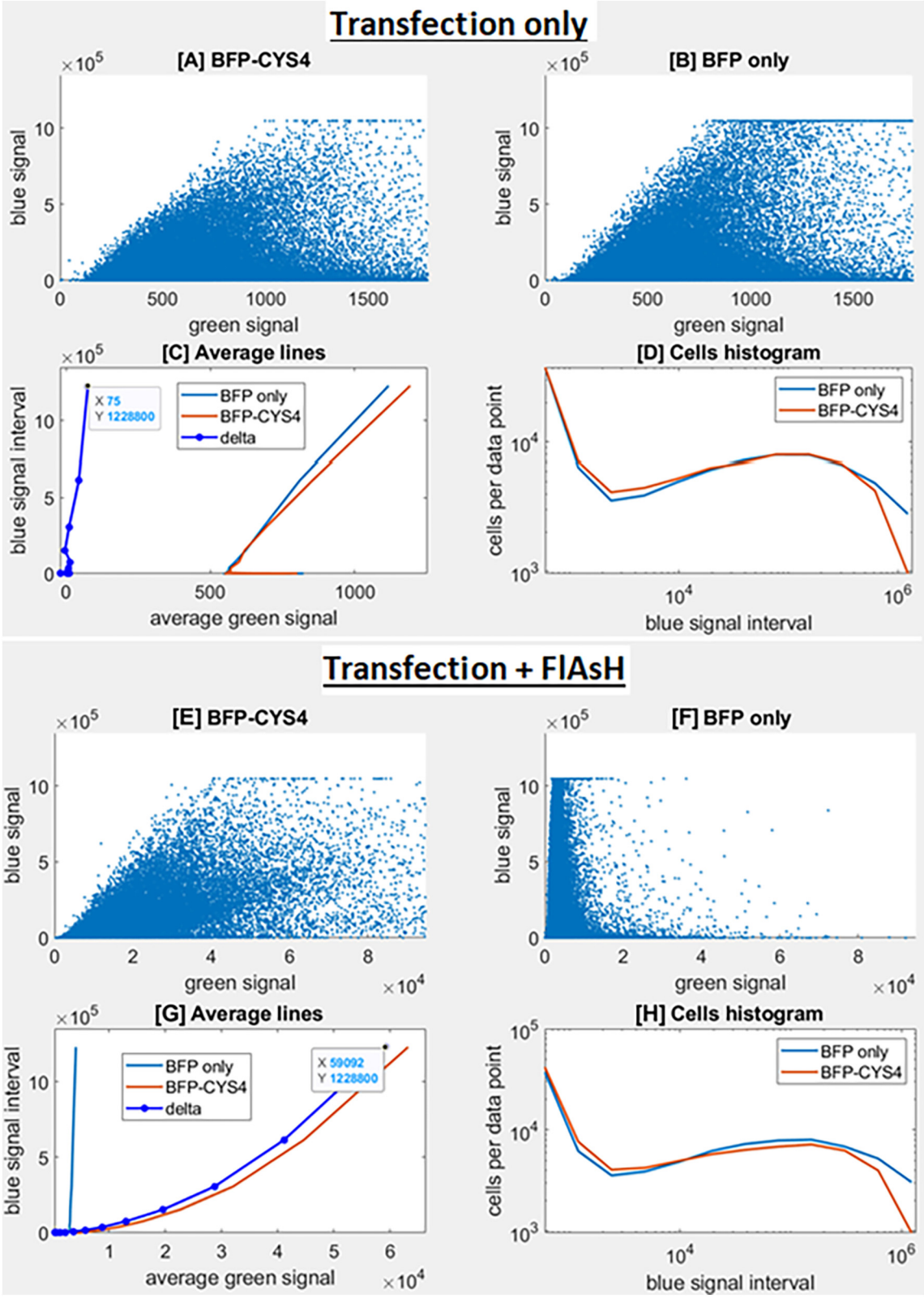

Fig. 1. (A and B) show the dot plot on a linear scale from transfected HeLa cells. Each dot represents the blue and green emission value of a single cell. (C) shows the average green value for each blue region, as well as the difference between them (delta). (D) shows a histogram of the number of cells in each blue region. (E–H) Cells expressing the BFP-CYS4 fusion protein and treated with FlAsH (a cell permeable version of CrAsH), showed a monotonous increase in green (FlAsH related) emission, with higher blue (BFP-CYS4 related) emission. On the contrary, the reference cells expressing BFP-only showed relatively no change. The delta line, showing the difference between the two curves, will be used as an indicator of CrAsH-CYS4 colocalization and nanocarrier cytosolic penetration.

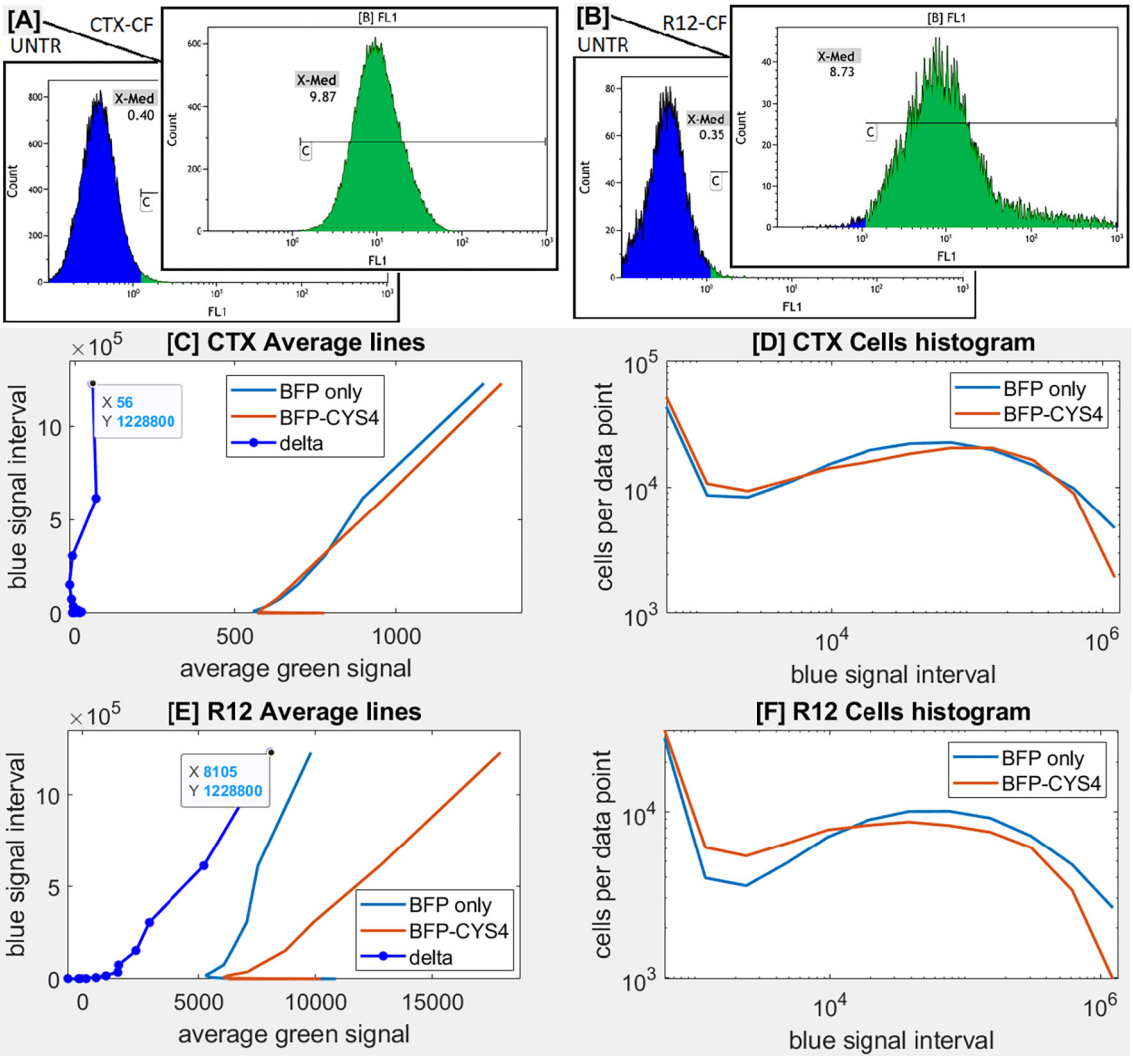

Fig. 2. R12 and CTX were first selected to demonstrate the assay, as positive and negative controls. A treatment protocol that maximises total cellular uptake was selected and tested using Carboxy-fluorescein conjugates. A and B show the total uptake in the selected protocols – 15 μM R12 for 15 min, and 15 μg*mL^{-1} for CTX for 1.5 h. C and D show the same treatment conditions with CTX-CrAsH, and E and F for R12-CrAsH. For CTX, no significant difference in the delta line is observed, while for R12, the delta line value increases monotonously with higher BFP-CYS4 expression levels, indicating high levels of cytosolic penetration.

Table 1
HeLa cells penetration by different drug nanocarriers. The signal is taken as the value of the delta line, in the highest blue region. On/Off ratio was measured ex-cellulo with free CYS4. Relative total delivery was obtained by dividing the signal by the degree of labelling (DOL) and by the On/Off ratio. For PEI DOL is per polymer of 25 kDa. For PMDA DOL is per micelle of (estimated) 3800 monomers. For Cationic liposomes encapsulated DNA DOL is per plasmid DNA molecule of 1.4 MDa.

Vector	Signal ± SD	*Z*-factor	Degree of labelling	Ex-cellulo on/off ratio	Relative total delivery	Penetration ratio [%]	Method (cell treatment protocol)	Comparison to literature
R12	7192 ± 649	0.71	0.17	53 ± 4	813	1.5 ± 0.2	15 μM, 15 min incubation, followed by 1 h post incubation	Qualitative [14,15]
25 kDa PEI	1940 ± 194	0.638	2.9	46 ± 2	14.8	1.55 ± 0.2	16.2 μg*mL^{-1}, 2 h incubation	Penetration ratio < 10 % [13]
HFn	2492 ± 199	0.71	6	10.1 ± 0.9	45.6	13 ± 2	40 μg*mL^{-1}, 2 h incubation	Qualitative [28]
PMDA	2436 ± 239	0.66	0.42	24 ± 9	252	5 ± 2	0.8 mM monomer, 2 h incubation	Qualitative [29]
Cationic liposomes	4946 ± 292	0.8	32	33 ± 1	4.7	3.6 ± 0.6	60 μg*mL^{-1} DNA, complexed with 15.6 μg*mL^{-1} protamine, 2 h incubation	Qualitative [12]
CTX	73 ± 64	–	7	6.2 ± 0.7	2	0.7 ± 1.5	15 μg*mL^{-1}, 1.5 h incubation	–

Comparing the cytosolic penetration of R12 and CTX

Next, HeLa cells transiently transfected with either BFP-CYS4 or BFP-only were treated using the same selected treatment protocol, with either R12-CrAsH or CTX-CrAsH, before being harvested and measured by flow cytometry (Fig. 2C–F).

Cells treated with R12-CrAsH show a gradually increasing delta line indicative of cytosolic localisation of CrAsH (Fig. 2E), qualitatively similar to the result obtained in Fig. 1G. In contrast, cells treated with CTX-CrAsH (Fig. 2C) did not show any substantial change in the delta line. A triplicate of the same R12-CrASH sample gave an average green signal (maximal value of the delta line) of 7192 ± 649. A triplicate of the CTX-CrAsH sample gave an average green signal of 57 ± 33.

To appreciate the utility of the assay, we calculated the *Z*-factor – comparing the signal generated by an assay's positive (high endosomal escape) and negative controls (low/no endosomal escape). A Z-factor between 0.5 and 1 is considered excellent. Using R12 as a positive control and CTX as a negative control of cytosolic delivery, we calculated a Z-factor [12] higher than 0.7 (see Table 1, and SI), indicating an excellent assay of R12 cellular penetration.

A different way to look at the data could use the same maximal green emission, as well as the background auto-fluorescence of the cells, to calculate the fraction of nanocarrier in the cytoplasm, out of the total associated to the cell. The emission of cells with high expression of BFP-only, or BFP-CYS4, is expressed by Eqs. (7) and (8), respectively.

$$I_{BFP-only} = 2.303 * I_0 * \varepsilon * l * C^{Total} * QY^{off} + background \quad (7)$$

$$I_{BFP-CYS4} = 2.303 * I_0 * \varepsilon * l * \left(C^{cytosol} * QY^{on} + C^{rest} * QY^{off}\right) + background \quad (8)$$

After subtracting the autofluorescence (as measured for transfected cells not treated with CrAsH), we have the ratio in Eqs. (9) and (10).

$$\frac{I_{BFP-CYS4} - background}{I_{BFP-only} - background} = \frac{C^{cytosol}}{C^{Total}} * \left(\frac{QY^{on}}{QY^{off}} - 1\right) + 1 \quad (9)$$

$$penetration\ ratio\ (\%) = 100 * \frac{C^{cytosol}}{C^{Total}} = 100 * \frac{\frac{I_{BFP-CYS4} - background}{I_{BFP-only} - background} - 1}{\left(\frac{QY^{on}}{QY^{off}} - 1\right)} \quad (10)$$

We assume here that CrAsH emission in both states is stable, however, plausible quenching of CrAsH in endosomes/lysosomes could give a false increase in calculated penetration ratio (such quenching should have no effect on Eqs. (1)–(6)).

This way, using the emission values 1076, 1159, 9990, and 17,183, for BFP only, BFP-CYS4, BFP only treated with R12-CrAsH, and BFP-CYS4 treated with R12-CrAsH respectively (these are triplicate averages, one replicate of which is presented in Figs. 1C and 2E, see also SI), we calculated 1.5 ± 0.2 % cytosolic delivery of R12. Likewise, for CTX we calculated 0.7 ± 1.5 % in HeLa cells (see Table 1 and SI).

Expansion to other drug delivery agents

Using the same method, we obtained the results in Table 1, for the cytosolic penetration of HFn, PMDA, PEI, and cationic liposomes, all with an excellent *Z*-factor and statistical significance (see SI for uptake and complete CrAsH signal). When comparing the data of different nanocarriers, special attention should be given to the cell treatment protocol chosen, which does not always maximize the delivery. Indeed, the uptake of the cationic liposomes and HFn can be increased with higher dose or longer incubation time. On the contrary, the uptake of other nanocarriers was increased up to the toxicity limit: R12 (toxicity was evident by morphology change and loss of adhesion within 1 h of incubation), PEI (see SI for MTT assay), and PMDA [20] were all used just below their own toxicity limit. Also, differences in definition of labelling ratio (e.g., for cationic liposomes), and possible drug loading potential need to be accounted for. That considered, some nanocarriers greatly outperformed others, either in terms of total delivery (R12) or by penetration ratio (HFn).

PEGylation impact on HFn cytosolic delivery

One drug nanocarrier of interest in our lab is HFn; for this reason, HFn was selected to demonstrate the utility of this assay, and to further explore its cell penetration ability. Our question was – does PEGylation of HFn affect its cell penetration? To answer this question, a sample of HFn was labeled with CrAsH, and later divided and treated with 5 kDa methoxyPEG-NHS at 0, 1, and 5 mM. This test (Fig. 3) showed an increase in cell penetration of HFn with increased PEGylation. This might shed some light on HFn ability to penetrate cells as well as its mechanism of penetration.

Testing different cells

To use this method with different cell lines, the cells would have to be efficiently transfected and express the BFP-CYS4 fusion protein, and resist the mandatory chemicals / procedures (e.g., repeated washing, BAL). To test this, we chose T98G cells, PMDA-CrAsH as a drug nanocarrier, and CTX-CrAsH as negative control (Fig. 4). First an uptake experiment was done using carboxyfluorescein-conjugated PMDA (PMDA-CF) and CTX (CTX-CF), and a treatment protocol was optimized such that both nanoconjugates showed high cellular uptake (Fig. 4A–B). This treatment protocol was then used to test PMDA-CrAsH and CTX-CrAsH (Fig. 4E–H). The T98G cells had a lower expression level of BFP-CYS4 (compared to HeLa cells), but that level was sufficient for a comparison of the two nanoconjugates. A clear cytosolic penetration signal was evident from PMDA (Fig. 4G and H), very similar to the result in HeLa cells. The signal of CTX-CrAsH (Fig. 4E and F) was substantially lower, and could be understood as a marginal cytosolic penetration signal, or simply as noise, probably the result of less cells counted with high BFP expression (see cell histograms). The

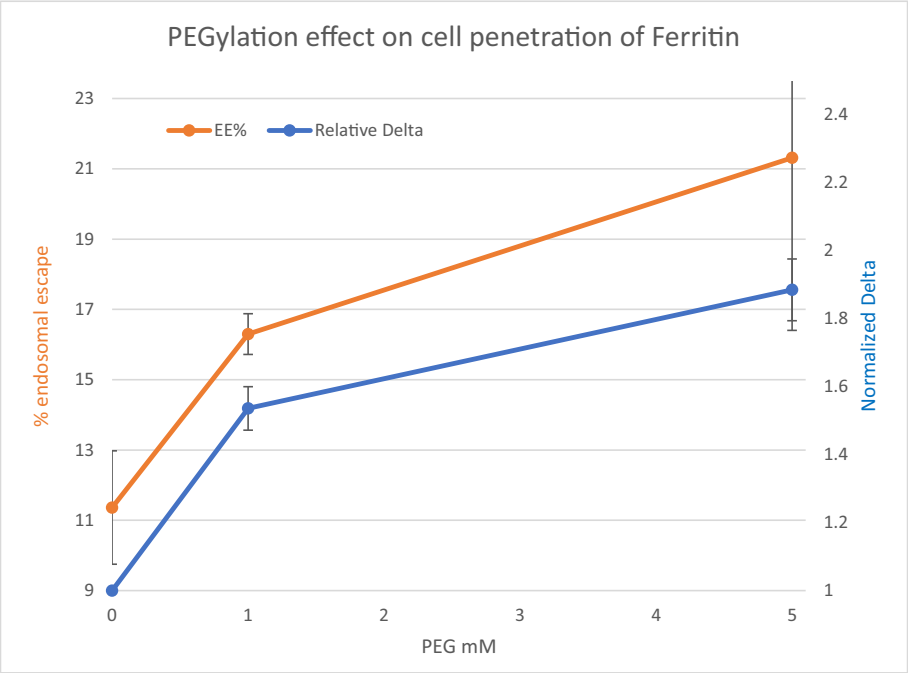

Fig. 3. PEGylation was found to increase cell penetration, both in terms of delivery ratio and total amount. Each data point represents three independent experiments. The Delta signal from each experiment (delta green at max blue) was normalized to the non-PEGylated sample. Error bars represent one SD.

triplicate average values (delta line value in the maximal blue region) were 5184 ± 718 for PMDA, and 351 ± 138 for CTX, giving a *Z*-factor of 0.468. The penetration ratio was 6.1 ± 2.6 % and 6 ± 3 % respectively.

Discussion

So far, a widely accepted standard method to quantify endosomal escape is lacking. For this reason, there are only vague estimations of the performance of many drug nanocarriers, obtained using different methods in different publications. This limited the testing and development of better nanocarriers.

The purpose of this work was to develop a method to quantify endosomal escape and/or cytosolic penetration, based on the pro-fluorophore CrAsH, using BFP to quantify the transgene expression, and using a BFP-only as a reference to BFP-CYS4. If we assume that the On/Off ratio of the nanocarrier-CrAsH conjugate is unchanged inside the cell, that the uptake of the nanocarrier is the same on average in each blue region, and that at high BFP-CYS4 expression levels cytoplasmic CrAsH binding is complete, then Eqs. (1)–(10) hold, and we expect the delta line to look like a vertical saturation curve. The delta curves obtained for most nanocarriers seems to resemble that expectation (see Figs. 2, 4, and the SI).

In this way, we managed to obtain a statistically robust signal from a variety of potential drug nanocarriers, utilizing a variety of cell penetration mechanisms. This was also applied to explore and improve the cytosolic delivery of the bionanoparticle HFn and demonstrated with a different cell line.

In Table 1 we compared the performance of different nanoparticles to penetrate the cytoplasm of HeLa cells, which served as a model cell line for this study. We did not account for different cell penetration kinetics and different treatment protocols, which were chosen from the literature solely based on allowing sufficient uptake and statistical significance. This point could also have an effect as the CrAsH signal was found to be transient and, in some cases, substantially diminished within an hour, which might reflect cellular metabolic processes that eliminate the nanocarrier and/or CrAsH. Some insight however can be gained by the vast differences in cytoplasm penetration performances, as reflected by the assay (Table 1), in terms of total delivery and penetration/association ratio.

We hope this work will enable in depth exploration of parameters such as drug loading and chemical modifications and their impact on cytosolic drug delivery, and help the development of new drug delivery agents. See comparison to other notable methods in SI.

Materials and methods

Reagents

Oak Ridge Teflon tubes, n-hydroxy succinimide (NHS), dichloromethane, carboxyfluorescein (CF), DMSO, Diisopropylcarbodiimide (DIC), MeOH, triethylamine (TEA), acetic acid, toluene, MOPS, Tris(2-carboxyethyl)phosphine hydrochloride (TCEP), NaOH, BAL, Poly(isobutylene-alt-maleic anhydride), dodecylamine, THF, chloroform, boric acid, 2,2′-(Ethylenedioxy)bis(ethylamine), N-(3-Dimethylaminopropyl)-N′-ethylcarbodiimide hydrochloride (EDC), amicon centrifugal filters, Ethanol, Polyethylenimine (PEI) 25 kDa, piperidine, were all purchased from Sigma-Aldrich.

Zeba 7kd size exclusion columns, Bradford (Coomassie plus), DMEM, FBS (fetal bovine serum), penicillin-streptomycin, L-glutamine, EDTA, trypsin-EDTA, PBS, PBS supplemented with

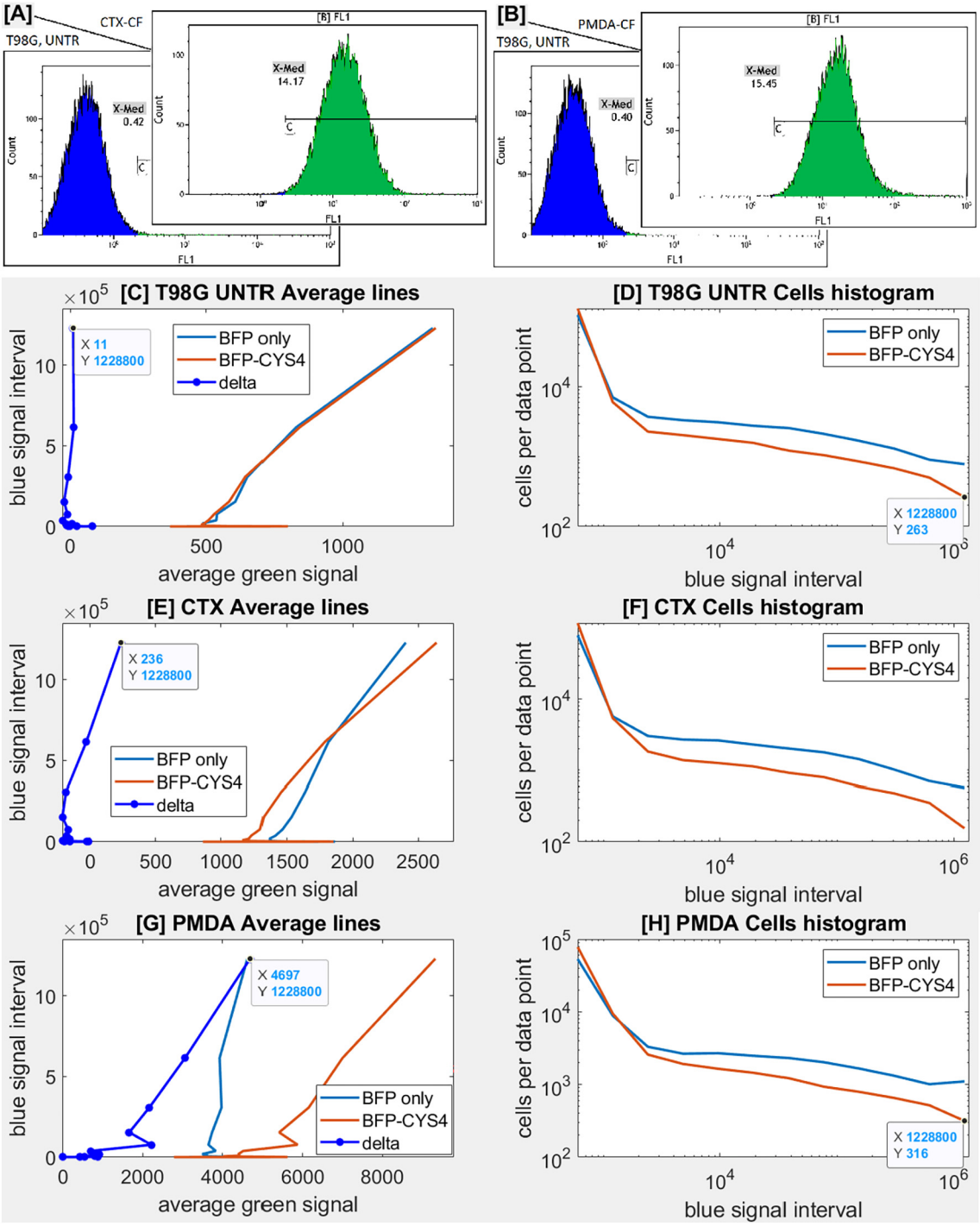

Fig. 4. Quantifying the cytosolic penetration of PMDA in T98G cells. [A] and [B] show the total uptake of PMDA-CF and CTX-CF (as negative control). The same treatment protocols were used for [E] and [G], with CrAsH instead of CF. [C] and [D] show the average line (average green value per blue region) and blue intensity histogram of transfected only (no CrAsH) T98G cells. In [E] and [F] cells were treated with CTX-CrAsH. Contrary to HeLa cells, a small degree of CTX endosomal escape was evident. In [G] and [H] cells were treated with PMDA-CrAsH, and a clear endosomal escape signal was evident, similar to HeLa cells.

calcium and magnesium, Lipofectamine 3000 transfection reagent were all purchased from ThermoFisher.

FlAsH-EDT2 wash purchased from Cayman Chemical.

Cetuximab was kindly gifted by prof. Fabio Corsi, ICS Maugeri, Pavia, Italy.

Cloning

The pcDNA3 plasmid backbone has been obtained from pcDNA3-EGFP vector (Addgene plasmid #13031). EGFP gene has been excided from the plasmid using XhoI-XbaI restriction

sites and replaced with the coding sequence of the aminoacidic CrAsH target sequence (FLNCCPGCCMEP) [30,31] in the same position. Plasmid construction by annealed oligo cloning: forward 5′-PHO-TCGAGTTTCTTAATTGCTGCCCCGGGTGCTGCATGGAACCTTAA**GGTACCCTCGAG**TAAT-3′, added digested XhoI (at the beginning) and XbaI (at the end) restriction sites (underlined); reverse 5′-PHO-CTAGATTA**CTCGAGGGTACC**TTAAGGTTCCATGCAGCACCCGGGGCAGCAATTAAGAAAC-3′, added digested XbaI (at the beginning) and XhoI (at the end) restriction sites (underlined); added additional restriction sites (KpnI, XhoI) into the sequence (bold); primers were modified by a 5′-terminal phosphorylation (PHO).

EBFP2 gene sequence has been amplified by PCR (with primers: forward 5′-ATTAGGATCCACCATGGTGAGCAAGGGCGAGGA-3′, added BamHI restriction site underlined; reverse 5′- AATTAGAATTCCTTGTACAGCTCGTCCATGCCGAGA-3′, added EcoRI restriction site underlined) from the EBFP2-C1 vector (Addgene plasmid #54665).

The EBFP2 gene has been cloned into the previously described pcDNA3-CrAsH-target vector, using BamHI-EcoRI restriction sites, to obtain a pcDNA3-EBFP2-CrAsH-target (from now on called BFP-CYS4).

As control plasmid, a pcDNA3-EBFP2 (called BFP-only) has been obtained exciding the CrAsH-target sequence from the BFP-CYS4, by XhoI digestion.

Cell growth and transfection

HeLa and T98G cell lines were cultured using complete medium: DMEM (Euroclone), supplemented with 10 % fetal bovine serum (FBS), 1 % penicillin-streptomycin, 1 % L-glutamine.

HeLa cells (2.5×10^5/well) and T98G cells (3×10^5/well) were plated in 12-well plate and transfected after 24 h with Lipofectamine 3000 (ThermoFisher) with 1 μg of DNA plasmid (BFP-CYS4 or BFP-only) in each well, in accordance to the datasheet.

Up-take experiments

HeLa cells (2.5×10^5/well) and T98G cells (3×10^5/well) were plated in 12-well plate. After 48 h from seeding, the cells have been incubated with each nanocarrier, marked with carboxy-fluorescein. After the incubation time, cells were washed with PBS and incubated with 300 μL of trypsin-EDTA for 3 min at 37 °C; after the addition of 1 mL of complete medium, cells were collected in tubes. Then, cells were centrifugated (200 ×g for 3 min), washed once with PBS, centrifugated again, resuspended in 300 μL of PBS-EDTA (2 mM) and analyzed by flow cytometry (Gallios, Beckman Coulter), using 488 nm laser and 525/20 nm filter.

FlAsH and CrAsH experiments

After 24 h from transfection, cells were washed twice with PBS (supplemented with calcium and magnesium; from now on called $PBS^{+Ca,Mg}$) and incubated in DMEM supplemented with 500 nM free-FlAsH [31] for 1 h or nanocarrier-CrAsH (Cationic liposomes encapsulated DNA at 60 μg*mL^{-1} DNA 450uL for 2 h, PEI 15 μg*mL^{-1} 500 μL for 2 h; polyArg 15 μM 350 μL, for 15 min, followed by another 1 h in only DMEM; ferritin 40 μg*mL^{-1} 400 μL for 2 h; PMDA 0.8 mM 500 μL for 2 h; CTX 15 μg*mL^{-1} 500 μL for 1 h and 30 min), at 37 °C in the chemical hood. After nanocarrier incubation, cells were incubated with $PBS^{+Ca,Mg}$ + BAL (200 μM) for 10 min at 37 °C and washed twice with $PBS^{+Ca,Mg}$. Cells were treated with 250 μL of trypsin-EDTA diluted 1:3 in PBS-EDTA (2 mM) for 2 min at 37 °C; treatment with trypsin time increased to 12 min for HeLa cells incubated with PMDA. After the addition of 900 μL of complete medium, cells were collected in tubes. Then, cells were centrifugated (200xRCF for 3 min), washed once with PBS, centrifugated again, resuspended in 450 μL of PBS-EDTA (2 mM) and analyzed by flow cytometry (Gallios, Beckman Coulter), with 405 and 488 nm lasers, and a 450/50 nm and 525/20 nm filters.

A typical experiment with a single sample would use one 12 well plate. A triplicate treated with the drug delivery agent for BFP-only and BFP-CYS4 cells (6 wells), a duplicate of transfected cells without the drug delivery agent (4 wells), and a duplicate of untreated untransfected cells (2 wells).

To calculate the *Z*-factor, the delta was calculated separately for the three triplicates, to give an average and standard deviation. To calculate the error of the penetration ratio, an average and standard deviation of the replicates were calculated first, and the error was propagated throughout the calculation.

R12 and CYS4 peptide synthesis

Peptides were assembled by stepwise microwave-assisted Fmoc-SPPS on a Biotage ALSTRA Initiator+ peptide synthesizer, and the collected crude peptides were then purified by preparative RP-HPLC on a Phenomenex Jupiter 10 μ C18 90 Å (250 × 21.2 mm) column. LC-MS was then run to characterize the purified fractions, which were then combined and lyophilized.

R12-dye conjugation

To a Teflon tube add 290 μL NHS in DCM 1.5 mM, 4.11 μL CF or CrAsH in DMSO 25.17 mM, and 11.38 μL DIC in DCM 18.2 mM. Incubate at 30 °C for 24–48 h. Test reaction progress in TLC with 10 % MeOH in DCM as mobile phase. Add 9.84 μL Triethylamine, 2.83 μL Acetic Acid, and 36 μL R12 in DMSO 2 g*L^{-1}. Incubate at 4 °C for 3 days. Test reaction progress in TLC with 100 % MeOH as mobile phase.

Cleaning

Move solution to 1.5 mL Eppendorf and evaporate DCM using Argon. Add 1.26 mL toluene, 44 μL Triethylamine, 10.8 μL Acetic Acid. Centrifugate at 1500 RCF for 1 Hour at 15 °C. Trash SUP. Add 1.26 mL toluene and centrifugate again for 5 min. Trash SUP. Evaporate leftover liquid under vacuum at 20 °C. Add 775 μL milliQ water, 15 μL MOPS buffer pH 7 0.4 M, 6.34 μL TCEP 240 mM (in 0.76 M NaOH), and 3 μL BAL 50 mM. Quantify final concentration using the Bradford assay.

PMDA synthesis

following a previously published procedure [20], poly [isobutene alt-maleic anhydride] was reacted with 75 % mole ratio of dodecylamine in THF at 65 °C for 4 h. The solvent was then partially evaporated under vacuum and let react further overnight. The solvent was completely evaporated and the polymer redissolved in Chloroform at 0.5 M (monomer).

PMDA phase transfer and EDBE functionalization

100 μL PMDA solution in chloroform was evaporated and 2 mL NaOH 50 mM was added. Solution was sonicated for 5 min until clear, and filtered 4 times using a sodium borate buffer pH 9 10 mM, and a 100 kDa centrifugal filter (total solvent dilution of 1/800 k), and obtain a suspension in water of 50 mM polymer.

Add 15 μL EDBE in milliQ 0.1 M, and 8 additions of 10 μL EDC 0.2 M every 15 min. After last addition let react for another 2 h at RT. Remove excess reactants by filtering twice using a 30 kDa filter and borate buffer pH 9 10 mM (total dilution 1/900). Final polymer concentration between 100 and 200 mM.

PMDA-dye conjugation

In a Teflon tube add 373 μL NHS in DCM 1.5 mM add 3.97 μL CF or CrAsH in DMSO 25.17 mM and 10.96 μL DIC in DCM 18.2 mM. incubate at 30 °C for 24–48 h. Evaporate DCM using Argon in RT and add 50 μL PMDA-EDBE 200 mM. Incubate at 4 °C overnight. Remove excess dye by filtration using a 10 kDa filter. Filter twice in water, twice in 50 % ethanol/water, and twice more in 10 mM MOPS buffer pH 7. Concentrate to 100–200 μL. Add 1 μL BAL 25 mM and 1.3 μL TCEP 240 mM (in 760 mM NaOH).

HFn nanocage design

As described in Bellini et al. [32], HFn was expressed and purified from BL21(DE3) *E. coli*.

Ferritin-Dye conjugation

In a Teflon tube, add 300 μL NHS in DCM 1.5 mM, add 2.72 μL CF or CrAsH in DMSO 25.17 mM, and 7.5 μL DIC in DCM 18.2 mM. incubate at 30 °C for 24–48 h. Evaporate solvent using Argon at RT, and add 71.3 μL Ferritin in PBS 1.9 $g*L^{-1}$ and 15 μL borate buffer pH 9, 0.1 M. incubate overnight at 4 °C. Dilute to 4 mL with PBS and reconcentrate using a 100 kDa filter (555 RCF). Then use a 0.5 mL Zeba 7 kDa size exclusion column (pre-equilibrated with 20 mM MOPS buffer pH 7.2 and 123 mM NaCl). Add 1.1 μL BAL 50 mM and 2 μL TCEP 240 mM (in 760 mM NaOH).

PEI 25 kDa dye conjugation

To a glass vial add 200 μL MOPS buffer pH 7.35 100 mM, 10 μL PEI in DMSO 10 $g*L^{-1}$, 3.2 μL CrAsH in DMSO 5 mM, 100 μL piperidine 0.5 M (in 0.5 M HCl). Add 150 μL EDC 0.2 M and incubate overnight at 4 °C. Wash using a 10 kDa filter with a solution of 8.5 mM piperidine, 8.5 mM HCl, in 2 mM borate buffer pH 9 to remove unconjugated dye, then wash again with borate buffer only to remove piperidine. Add 1 μL BAL 50 mM and 2 μL TCEP 240 mM (in 760 mM NaOH). To quantify PEI [33], add PEI to 143 μL 0.9 mM CuSO4 solution in 100 mM acetate buffer pH 5.4, and dilute to final volume of 0.2 mL and final PEI concentration of 15 $\mu g*mL^{-1}$. Measure absorption at 280 nm.

CTX-dye conjugation

To Teflon tube add 146.6 μL NHS in DCM 1.5 mM, add 1.33 μL CF or CrAsH in DMSO 25.17 mM, add 3.68 μL DIC in DCM 18.2 mM. Incubate at 30 °C 24-48H. Evaporate DCM using Argon at RT and add 12.5 μL borate buffer pH 9, 100 mM and 58 μL CTX in PBS 4.3 $g*L^{-1}$. Incubate at 4 °C overnight. Dilute to 4 mL in PBS and reconcentrate using a 50 kDa filter, then clean using a 0.5 mL Zeba 7 kDa size exclusion column (pre-equilibrated with MOPS buffer pH 7, 20 mM and 123 mM NaCl). Add 1.1 μL BAL 50 mM and 2 μL TCEP 0.24 M (in 0.76 M NaOH).

Cationic liposomes and lipid-protamine-DNA nanoparticles were produced following a previously published protocol [34] with some modifications. 1,2-dioleoyl-3-trimethylammonium-propane (DOTAP, Avanti Polar Lipids Inc., AL, US) and cholesterol (Sigma-Aldrich SRL) were dissolved in chloroform with 1:1 M ratio and the solvent was evaporated under reduced pressure. The lipid-film was then hydrated overnight with MilliQ water obtaining a final reagents concentration of 10 mM. After 20 min of bath sonication, the extrusion was performed using Avanti® Mini Extruder sequentially equipped with Whatman® polycarbonate membranes of 800, 200, and 100 nm (15 cycles/membrane).

Protamine-CrAsH conjugation

To 500 μL milliQ water add 25 μL protamine in PBS 5 $g*L^{-1}$, 5 μL CrAsH in DMSO 19.6 mM, and 30 μL EDC 1 M in borate buffer pH 9, 50 mM. incubate for 6 h at 4 °C. Concentrate sample under vacuum and add 100 μL acetate buffer 0.1 M, pH 5, in 154 mM NaCl, to final volume 110–130 μL. Remove excess reagents using a 0.5 mL Zeba 7 kDa size exclusion column pre-equilibrated with the same buffer. Protamine was quantified using the Bradford assay.

Mix 160 μg DNA with 41.6 μg Protamine-CrAsH in a total volume of 640 μL. Mix well and incubate at RT for 10 min. Sample 40 μL to test ex-cellulo activation. To the remaining 600 μL add 180 μL cationic liposomes, mix well and incubate at RT for 10 min. Add 120 μL Glucose 10 % in PBS.

Ex-cellulo activation

to test the On/Off emission ratio, in a 96 well plate, at a final volume of 200 μL per well, add the NP-CrAsH conjugate at a CrAsH final concentration 0.15 μM, MOPS buffer 20 mM pH 7.35 and Glutathione at 8 mM. Measure emission and add 1 μL CYS4 to a final concentration 10 μM. Incubate at 37 °C for 1 h before measuring emission at 532 nm, exciting at 518 nm.

CrAsH was synthesized according to a published protocol [35].

CRediT authorship contribution statement

R.R. designed the research, prepared the nanocarrier-crash conjugates, carried out the experiments, analyzed the data, and wrote the first draft; J.A.B. designed the plasmids, handled the cells, carried out the experiments, and provided advice on the draft writing; L.S. L.B. and M.A.R. provided some of the nanocarriers and critical advice; V.T. helped in the sample and cell handling; A.G. synthesized the peptides; S.A. synthesized the CrAsH fluorophore and provided critical advice; M.C. and D.P. designed the research, discussed the results, provided funding and wrote the manuscript.

All original data can be made available upon request.

Declaration of competing interest

The authors declare that they have no competing interests.

Acknowledgments

This work has received funding from AIRC under IG 2018 - ID. 21565 project – P.I. Prosperi Davide. Support to this work was also provided by Regione Lombardia POR FESR 2014-2020 (Call HUB Ricerca ed. Innovazione: ImmunHUB) and by MIUR (PRIN 2017, ID 2017E3A2NR project).

Appendix A. Supplementary data

Supplementary data to this article can be found online at https://doi.org/10.1016/j.nano.2022.102626.

References

1. Xiao Y, Shi J. Lipids and the emerging RNA medicines. *Chem Rev* 2021;**121**:12109-11, https://doi.org/10.1021/ACS.CHEMREV.1C00778.
2. Akinc A, Zumbuehl A, Goldberg M, Leshchiner ES, Busini V, Hossain N, et al. A combinatorial library of lipid-like materials for delivery of RNAi therapeutics. *Nat Biotechnol* 2008;**265**(26):561-9, https://doi.org/10.1038/nbt1402.
3. Elloumi HZ, Maharshak N, Rao KN, Kobayashi T, Ryu HS, Mühlbauer M, et al. A cell permeable peptide inhibitor of NFAT inhibits macrophage cytokine expression and ameliorates experimental colitis. *PLoS One* 2012;**7**, https://doi.org/10.1371/JOURNAL.PONE.0034172.
4. Zuppone S, Assalini C, Minici C, Bertagnoli S, Branduardi P, Degano M, et al. The anti-tumoral potential of the saporin-based uPAR-targeting chimera ATF-SAP. *Sci Reports* 2020;**101**(10):1-12, https://doi.org/10.1038/s41598-020-59313-8.
5. Selby LI, Cortez-Jugo CM, Such GK, Johnston APR. Nanoescapology: progress toward understanding the endosomal escape of polymeric nanoparticles. *Wiley Interdiscip Rev Nanomed Nanobiotechnol* 2017;**9**, https://doi.org/10.1002/wnan.1452.
6. Beddoes CM, Case CP, Briscoe WH. Understanding nanoparticle cellular entry: a physicochemical perspective. *Adv Colloid Interface Sci* 2015;**218**:48-68, https://doi.org/10.1016/j.cis.2015.01.007.
7. Zhao J, Stenzel MH. Entry of nanoparticles into cells: the importance of nanoparticle properties. *Polym Chem* 2018;**9**:259-72, https://doi.org/10.1039/c7py01603d.
8. Varkouhi AK, Scholte M, Storm G, Haisma HJ. Endosomal escape pathways for delivery of biologicals. *J Control Release* 2011;**151**:220-8, https://doi.org/10.1016/J.JCONREL.2010.11.004.
9. Hillaireau H, Couvreur P. Nanocarriers' entry into the cell: relevance to drug delivery. *Cell Mol Life Sci* 2009;**66**:2873-96, https://doi.org/10.1007/s00018-009-0053-z.
10. Martens TF, Remaut K, Demeester J, De Smedt SC, Braeckmans K. Intracellular delivery of nanomaterials: how to catch endosomal escape in the act. *Nano Today* 2014;**9**:344-64, https://doi.org/10.1016/J.NANTOD.2014.04.011.
11. Deprey K, Becker L, Kritzer J, Plückthun A. Trapped! A critical evaluation of methods for measuring Total cellular uptake versus cytosolic localization. *Bioconjug Chem* 2019;**30**:1006-27, https://doi.org/10.1021/ACS.BIOCONJCHEM.9B00112.
12. Munson MJ, O'Driscoll G, Silva AM, Lázaro-Ibáñez E, Gallud A, Wilson JT, et al. A high-throughput Galectin-9 imaging assay for quantifying nanoparticle uptake, endosomal escape and functional RNA delivery. *Commun Biol* 2021;**41**(4):1-14, https://doi.org/10.1038/s42003-021-01728-8.
13. Vermeulen LMP, Brans T, Samal SK, Dubruel P, Demeester J, De Smedt SC, et al. Endosomal size and membrane leakiness influence proton sponge-based rupture of endosomal vesicles. *ACS Nano* 2018;**12**:2332-45, https://doi.org/10.1021/acsnano.7b07583.
14. Wang T-Y, Sun Y, Muthukrishnan N, Erazo-Oliveras A, Najjar K, Pellois J-P. Membrane oxidation enables the cytosolic entry of polyarginine cell-penetrating peptides. *J Biol Chem* 2016;**291**:7902, https://doi.org/10.1074/JBC.M115.711564.
15. Kosuge M, Takeuchi T, Nakase I, Jones AT, Futaki S. Cellular internalization and distribution of arginine-rich peptides as a function of extracellular peptide concentration, serum, and plasma membrane associated proteoglycans. *Bioconjug Chem* 2008;**19**:656-64, https://doi.org/10.1021/BC700289W.
16. Lönn P, Kacsinta AD, Cui XS, Hamil AS, Kaulich M, Gogoi K, et al. Enhancing endosomal escape for intracellular delivery of macromolecular biologic therapeutics. *Sci Rep* 2016;**6**, https://doi.org/10.1038/srep32301.
17. Verdurmen WPR, Mazlami M, Plückthun A. A quantitative comparison of cytosolic delivery via different protein uptake systems. *Sci Rep* 2017;**7**, https://doi.org/10.1038/s41598-017-13469-y.
18. Teo SLY, Rennick JJ, Yuen D, Al-Wassiti H, Johnston APR, Pouton CW. Unravelling cytosolic delivery of cell penetrating peptides with a quantitative endosomal escape assay. *Nat Commun* 2021;**121**(12):1-12, https://doi.org/10.1038/s41467-021-23997-x.
19. Vermeulen LMP, De Smedt SC, Remaut K, Braeckmans K. The proton sponge hypothesis: fable or fact? *Eur J Pharm Biopharm* 2018;**129**:184-90, https://doi.org/10.1016/J.EJPB.2018.05.034.
20. Rotem R, Micale A, Rizzuto MA, Migliavacca M, Giustra M, Salvioni L, et al. Modeling the interaction of amphiphilic polymer nanoparticles with biomembranes to guide rational design of drug delivery systems. *Colloids Surf B Biointerfaces* 2020;**196**111366, https://doi.org/10.1016/j.colsurfb.2020.111366.
21. Pandolfi L, Bellini M, Vanna R, Morasso C, Zago A, Carcano S, et al. H-ferritin enriches the curcumin uptake and improves the therapeutic efficacy in triple negative breast cancer cells. *Biomacromolecules* 2017;**18**:3318-30, https://doi.org/10.1021/ACS.BIOMAC.7B00974/SUPPL_FILE/BM7B00974_SI_001.PDF.
22. Griffin BA, Adams SR, Tsien RY. Specific covalent labeling of recombinant protein molecules inside live cells. *Science (80-)* 1998;**281**:269-72, https://doi.org/10.1126/science.281.5374.269.
23. Adams SR, Tsien RY. Preparation of the membrane-permeant biarsenicals FlAsH-EDT2 and ReAsH-EDT2 for fluorescent labeling of tetracysteine-tagged proteins. *Nat Protoc* 2008, https://doi.org/10.1038/nprot.2008.144.
24. Cao H, Chen B, Squier TC, Mayer MU. CrAsH: a biarsenical multi-use affinity probe with low non-specific fluorescence. *Chem Commun* 2006, https://doi.org/10.1039/b602699k.
25. S C. Diffusion of proteins across the nuclear envelope of HeLa cells. *Biotechniques* 1998;**24**:668-74, https://doi.org/10.2144/98244RR04.
26. Rizzuto R, Brini M, Pizzo P, Murgia M, Pozzan T. Chimeric green fluorescent protein as a tool for visualizing subcellular organelles in

living cells. *Curr Biol* 1995;**5**:635-42, https://doi.org/10.1016/S0960-9822(95)00128-X.

27. Tanz SK, Castleden I, Small ID, Millar AH. Fluorescent protein tagging as a tool to define the subcellular distribution of proteins in plants. *Front Plant Sci* 2013:214, https://doi.org/10.3389/FPLS.2013.00214.
28. Bellini M, Riva B, Tinelli V, Rizzuto MA, Salvioni L, Colombo M, et al. Engineered ferritin nanoparticles for the bioluminescence tracking of nanodrug delivery in cancer. *Small* 2020;**16**:2001450, https://doi.org/10.1002/SMLL.202001450.
29. Marongiu L, Mingozzi F, Cigni C, Marzi R, Di Gioia M, Garrè M, et al. Inositol 1,4,5-trisphosphate 3-kinase B promotes Ca2+mobilization and the inflammatory activity of dendritic cells. *Sci Signal* 2021;**14**, https://doi.org/10.1126/SCISIGNAL.AAZ2120/SUPPL_FILE/AAZ2120_SM.PDF.
30. Martin BR, Giepmans BNG, Adams SR, Tsien RY. Mammalian cell-based optimization of the biarsenical-binding tetracysteine motif for improved fluorescence and affinity. *Nat Biotechnol* 2005, https://doi.org/10.1038/nbt1136.
31. Hoffmann C, Gaietta G, Zürn A, Adams SR, Terrillon S, Ellisman MH, et al. Fluorescent labeling of tetracysteine-tagged proteins in intact cells. *Nat Protoc* 2010;**510**(5):1666-77, https://doi.org/10.1038/nprot.2010.129.
32. Bellini M, Mazzucchelli S, Galbiati E, Sommaruga S, Fiandra L, Truffi M, et al. Protein nanocages for self-triggered nuclear delivery of DNA-targeted chemotherapeutics in cancer cells. *J Control Release* 2014;**196**:184-96, https://doi.org/10.1016/J.JCONREL.2014.10.002.
33. Ungaro F, De Rosa G, Miro A, Quaglia F. Spectrophotometric determination of polyethylenimine in the presence of an oligonucleotide for the characterization of controlled release formulations. *J Pharm Biomed Anal* 2003;**31**:143-9, https://doi.org/10.1016/S0731-7085(02)00571-X.
34. Salvioni L, Zuppone S, Andreata F, Monieri M, Mazzucchelli S, Di Carlo C, et al. Nanoparticle-mediated suicide gene therapy for triple negative breast cancer treatment. *Adv Ther* 2020;**3**:2000007, https://doi.org/10.1002/ADTP.202000007.
35. Adams SR, Campbell RE, Gross LA, Martin BR, Walkup GK, Yao Y, et al. New biarsenical ligands and tetracysteine motifs for protein labeling in vitro and in vivo: synthesis and biological applications. *J Am Chem Soc* 2002;**124**:6063-76, https://doi.org/10.1021/JA017687N/SUPPL_FILE/JA017687N_S1.PDF.